Whalen, D. L., Montemarano, J. A., Thakker, D. R., Yagi, H., & Jerina, D. M. (1977) *J. Am. Chem. Soc. 99*, 5522-5524.
Whalen, D. L., Ross, A. M., Yagi, H., Karle, J. M., & Jerina, D. M. (1978) *J. Am. Chem. Soc. 100*, 5218-5221.
Whalen, D. L., Ross, A. M., Montemarano, J. A., Thakker, D. R., Yagi, H., & Jerina, D. M. (1979) *J. Am. Chem. Soc. 101*, 5086-5088.
Wood, A. W., Wislocki, P. G., Chang, R. L., Levin, W., Lu, A. Y. H., Yagi, H., Hernandez, O., Jerina, D. M., & Conney, A. H. (1976) *Cancer Res. 36*, 3358-3366.
Wood, A. W., Chang, R. L., Levin, W., Yagi, H., Thakker, D. R., Jerina, D. M., & Conney, A. H. (1977) *Biochem. Biophys. Res. Commun. 77*, 1389-1396.
Yagi, H., Hernandez, O., & Jerina, D. M. (1975) *J. Am. Chem. Soc. 97*, 6881-6883.
Yagi, H., Thakker, D. R., Hernandez, O., Koreeda, M., & Jerina, D. M. (1977) *J. Am. Chem. Soc. 99*, 1604-1611.
Yang, L. L., Maher, V. M., & McCormick, J. J. (1982) *Mutat. Res. 94*, 435-447.
Yang, S. K., McCourt, D. W., Gelboin, H. V., Miller, J. R., & Roller, P. P. (1976) *J. Am. Chem. Soc. 99*, 1604-1611.
Yang, S. K., McCourt, D. W., & Gelboin, H. V. (1977) *J. Am. Chem. Soc. 99*, 5130-5134.

^{1}H NMR Studies on the Interaction between Distamycin A and a Symmetrical DNA Dodecamer†

Rachel E. Klevit,*,‡ David E. Wemmer,‡,§ and Brian R. Reid‡,∥
Departments of Chemistry and Biochemistry, University of Washington, Seattle, Washington 98195
Received November 6, 1985; Revised Manuscript Received January 21, 1986

ABSTRACT: High-resolution NMR techniques have been used to examine the structural and dynamical features of the interaction between distamycin A and the self-complementary DNA dodecamer duplex d-(CGCGAATTCGCG)$_2$. The proton resonances of d(CGCGAATTCGCG)$_2$ have been completely assigned by previous two-dimensional NMR studies [Hare, D. R., Wemmer, D. E., Chou, S. H., Drobny, G., & Reid, B. R. (1983) *J. Mol. Biol. 171*, 319-336]. Addition of the asymmetric drug molecule to the symmetric dodecamer leads to the formation of an asymmetric complex as evidenced by a doubling of DNA resonances over much of the spectrum. In two-dimensional exchange experiments, strong cross-peaks were observed between uncomplexed DNA and drug-bound DNA resonances, permitting direct assignment of many drug-bound DNA resonances from previously assigned free DNA resonances. Weaker exchange cross-peaks between formerly symmetry related DNA resonances indicate that the drug molecule flips head-to-tail on one duplex with half the frequency at which it leaves the DNA molecule completely. In experiments performed in H_2O, nuclear Overhauser effects (NOEs) were observed from each drug amide proton to an adenine C2H and a pyrrole H3 ring proton. In two-dimensional nuclear Overhauser experiments performed on D_2O solutions, strong intermolecular NOEs were observed between each of the three pyrrole H3 resonances of the drug and an adenine C2H resonance, with weaker NOEs observed between the drug H3 resonances and C1'H resonances. The combined NOE data allow us to position the distamycin A unambiguously on the DNA dodecamer, with the drug spanning the central AATT segment in the minor groove.

The sequence-specific recognition of DNA molecules by proteins and small molecules is an important component in the regulation of many biological processes. Two related antibiotics, netropsin and distamycin, have received much attention as models of sequence-specific, nonintercalative DNA-binding molecules. For the most part, physical studies to date have focused on the smaller netropsin molecule, and the results from such studies have been extended by analogy to the larger distamycin molecule. Studies involving exchangeable imino proton NOEs[1] (Patel, 1982) have been performed in solution on a complex of netropsin and the symmetric dodecamer d(CGCGAATTCGCG)$_2$; crystallographic studies on this complex have also been reported (Kopka et al., 1985). The recently published crystal structure of the netropsin-DNA complex confirms earlier proposals that the drug binds in the minor groove of B-form DNA and interacts specifically with AT base pairs.

We have used high-resolution ^{1}H NMR techniques to study the complex between distamycin and d(CGCGAATTCGCG)$_2$. The proton resonances of this DNA duplex have been completely assigned by previous two-dimensional NMR (2D NMR) experiments (Hare et al., 1983).

Materials and Methods

Sample Preparation. The DNA dodecamer was synthesized according to the solid-phase phosphite triester method as previously described (Hare et al., 1983). Distamycin A was obtained as the hydrochloride salt from Sigma. D_2O (99.996%

† This work was supported by NIH Grant GM-32681. The 500-MHz spectrometer is supported by instrumental grants from the Murdock Foundation, the National Science Foundation (PCM80-18053), and the National Institutes of Health (GM-28764-01S1).
‡ Department of Chemistry.
§ Present address: Department of Chemistry, University of California at Berkeley, Berkeley, CA 94720.
∥ Department of Biochemistry.

[1] Abbreviations: 2D NMR, two-dimensional nuclear magnetic resonance; NOE, nuclear Overhauser effect; NOESY, two-dimensional NOE spectroscopy; COSY, two-dimensional *J*-correlated spectroscopy; FID, free induction decay; 1D, one dimensional.

0006-2960/86/0425-3296$01.50/0

atom purity) was purchased from Aldrich. The total amount of DNA used in each NMR experiment was determined by UV absorbance at 260 nm. NMR samples were prepared by dissolving the dodecamer in 0.5 mL of 10 mM phosphate buffer (pH 7.0) and 10 mM NaCl and then lyophilizing the sample to dryness. For experiments performed in D_2O solution, the dried sample was redissolved in 0.5 mL of 99.996% atom purity D_2O. For experiments performed in H_2O solution, the sample was redissolved in 0.5 mL of 90% H_2O and 10% D_2O. A fresh stock solution of distamycin in the same phosphate buffer was prepared before each titration experiment.

NMR Spectroscopy. NMR spectra were obtained on a Bruker WM-500 spectrometer. Two-dimensional spectra (exchange and NOESY) were obtained in the phase-sensitive mode as described by States et al. (1982). The spectra were collected into 1024 complex points with quadrature detection. For each t_1 value, 64 scans were signal-averaged, with a recycle time of 2.3 s. The residual HDO signal, which was placed on-resonance, was saturated during the recycle time. Normally, around 300–400 t_1 experiments were collected.

The two-dimensional spectra were copied onto magnetic tape and transferred to a VAX 11/780 to be processed with in-house software developed by Dr. Dennis Hare. A sine bell window function, phase-shifted by 35° and skewed toward the beginning of the FID, was applied to the data prior to the t_2 Fourier transform. The data in t_1 were apodized with a sine bell that was phase-shifted by 35°. After transformation, the t_1 streaking was reduced when necessary by using the subtraction method (Klevit, 1985).

In the exchange experiments, cross-peak intensities were measured by integrating peaks of one-dimensional slices of the spectra. Average intensities were computed by taking the arithmetic average of the intensities of a single class of cross-peaks. To observe the exchangeable protons, spectra were obtained in 90% H_2O/10% D_2O solutions by using a modified Redfield 2–1–4–1–2 pulse.

Results

Titration of DNA with Distamycin A. Figure 1 shows the results of adding increasing amounts of distamycin to the dodecamer, d(CGCGAATTCGCG). Resonance assignments for the base protons of the four central AT base pairs have been reported elsewhere (Hare et al., 1983). The addition of the drug in less than stoichiometric amounts leads to a doubling of resonances over much of the spectrum. With increasing distamycin, resonances from the original dodecamer spectrum decrease (dashed lines), disappearing completely after the addition of 1.0 mol equiv (drug–DNA duplex), while new resonances increase (solid lines) in proportion to the amount of drug added. This effect is especially clear for the methyl resonance of T7 (the most upfield resonance in the spectrum) and for many of the aromatic base protons. The spectra shown in Figure 1 were obtained at 27 °C and exhibit slow-exchange behavior. When the temperature is increased, the spectrum of a partly saturated DNA sample becomes broader, indicating that the drug is exchanging between DNA molecules.

Assignments of the Nonexchangeable Protons: Two-Dimensional Exchange Experiments. From the behavior observed during the drug titration, we estimated that the off-rate for a distamycin molecule is in the range of 10–100 s^{-1}. Therefore, two-dimensional exchange experiments (Meier & Ernst, 1979) were performed on a sample of DNA to which 0.5 equiv of distamycin had been added. Figure 2 shows the aromatic and C1′H regions of an exchange spectrum obtained with a mixing time of 100 ms. The spectrum exhibits four

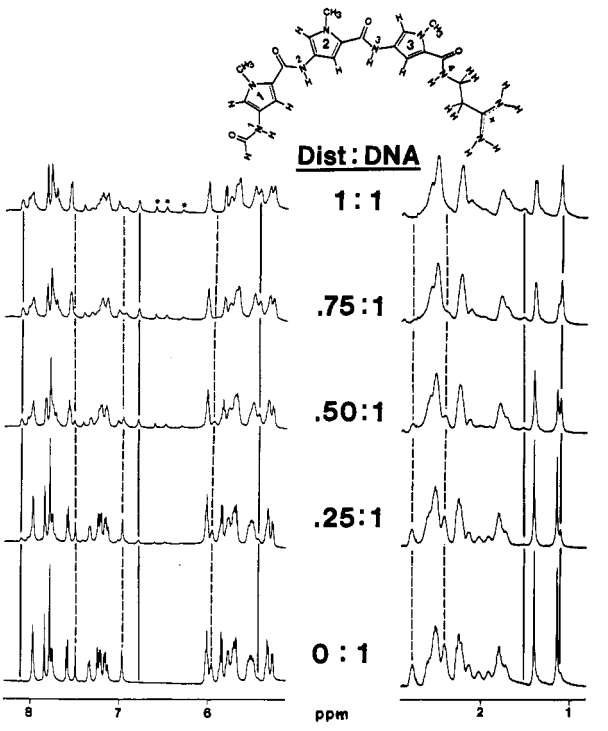

FIGURE 1: Titration of $d(CGCGAATTCGCG)_2$ with distamycin A. The aromatic and C1′H region (left) and the thymine methyl and C2′, C2″H region (right) of the 500-MHz NMR spectrum (27 °C) are shown with increasing amounts of distamycin added. The dashed lines follow some representative resonances that disappear from the spectrum with increasing drug, while the solid lines follow a few representative resonances that appear during the titration. The three peaks denoted with asterisks are from the three pyrrole H3's of the drug molecule (see text).

different types of exchange cross-peaks: (i) pairs of cross-peaks from a single diagonal peak, (ii) single cross-peaks that have the same intensity as the paired cross-peaks, (iii) single cross-peaks that have twice the intensity of the paired cross-peaks, and (iv) a much weaker set of cross-peaks. The first three types of peaks are all observed between resonances of the original DNA spectrum and resonances of drug–DNA complex, while the fourth type of cross-peak occurs between resonances of the complex. The paired cross-peaks arise because binding of the asymmetric distamycin molecule to the dodecamer destroys the symmetry of the DNA duplex. Thus, a resonance that belonged to two symmetry-related protons (one from each strand) in the free duplex splits into two resonances in the complex; resonances derived from residues A5, A6, T7, and T8 exhibit such behavior. The single cross-peaks arise from the same effect except that only one of the protons experiences a new chemical shift in the complex; an example is the cross-peak derived from the C5H resonance of C9. The third type of cross-peak arises when the two initially symmetrical protons have identical chemical shifts in the asymmetric complex, for instance, the C6H of T7 and C8H of G10. The fourth type of cross-peak arises from a "flip-flop" exchange, which will be discussed later. Since the spectrum of the free duplex has been completely assigned, the first three types of cross-peaks allow us to transfer those assignments to the spectrum of the drug–DNA complex, as illustrated in Figure 2 and summarized in Table I. Although resonances from residues C3 to C11 give exchange peaks, only those resonances from A5 through T8 give the double exchange peaks indicative of major asymmetric changes. Therefore, although the absolute chemical shift of protons outside the central four AT base pairs are affected by drug binding, the chemical shift "equivalence" of these protons is unaffected.

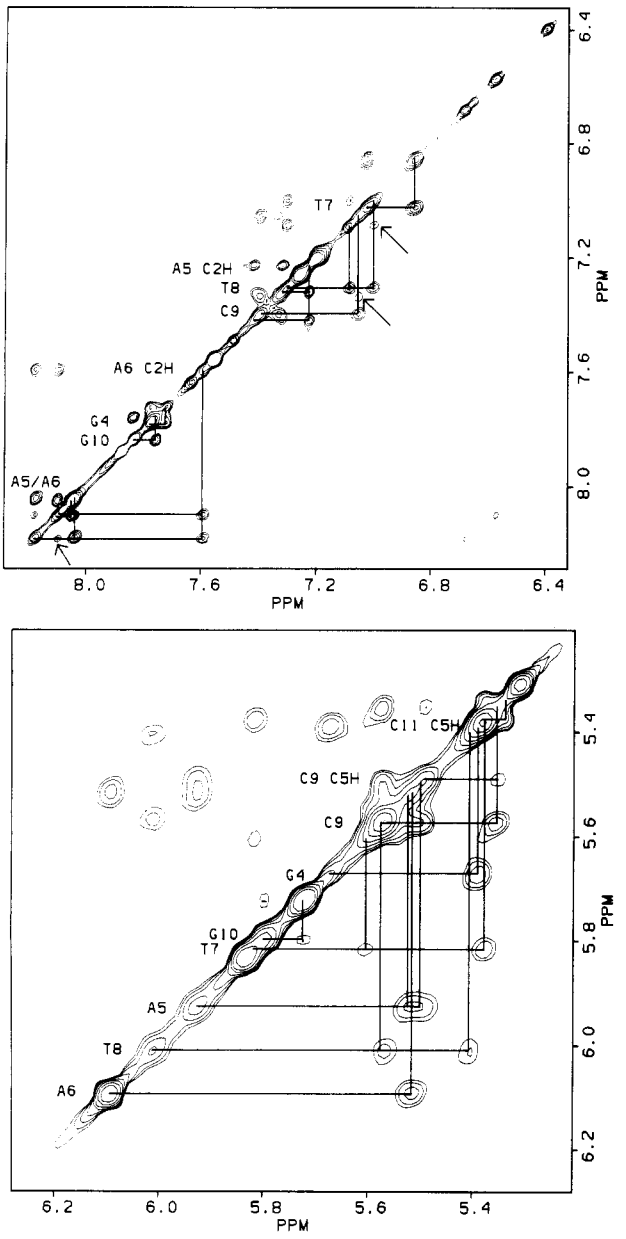

FIGURE 2: 2D exchange spectrum: the aromatic region (top) and the C1′H, C5H region (bottom) of an exchange spectrum of a half-saturated solution of dodecamer (drug:DNA duplex = 0.5:1). The spectrum shown was obtained with a mixing time of 100 ms at 27 °C. The resonance assignments given along the diagonal correspond to the assignments made on the free DNA dodecamer (Hare et al., 1983). The arrows in the top spectrum point to the flip-flop exchange peaks (see text).

Binding of distamycin to the dodecamer results in significant changes in chemical shifts throughout the spectrum. Although only the base protons and C1′ protons could be easily followed in the exchange experiment, analysis of the 1D spectra obtained through a drug titration reveals that changes occur in all regions of the spectrum. For those resonances that have been positively identified (Table I), we note that drug binding results in the largest shift differences for the central four AT base pairs. In addition, the C2H and C8H resonances of A5 and A6 are shifted downfield while all other affected protons are shifted upfield.

Once the DNA proton resonances in the spectrum have been identified from the exchange experiment, it is possible to identify resonances from drug pyrrole protons (three H3 and three H5 resonances). Three of these peaks are clearly resolved between 6 and 7 ppm and are marked with asterisks in the top spectrum of Figure 1. The other three pyrrole resonances appear in the more crowded aromatic region of the spectrum.

Table I: Chemical Shifts of DNA Resonances in the Presence and Absence of Distamycin A

proton	chemical shifts (ppm) −distamycin	+distamycin	Δδ
C1 C6H	7.55	7.55	0.00
G2 C8H	7.88	7.88	0.00
C3 C6H	7.20	7.20	0.00
G4 C8H	7.78	7.72	0.06
G4 C1′H	5.67	5.39	0.28
A5 C8H	8.05	8.10	−0.05
A5 C2H	7.22	7.32	−0.10
		7.42	−0.20
A5 C1′H	5.93	5.51	0.42
A6 C8H	8.04	8.04	0.00
		8.18	−0.14
A6 C2H	7.59	8.10	−0.51
		8.18	−0.59
A6 C1′H	6.09	5.51	0.58
T7 C6H	7.02	6.86	0.16
T7 C1′H	5.82	5.60	0.22
		5.37	0.45
T8 C6H	7.31	7.08	0.23
		7.00	0.31
T8 C1′H	6.01	5.56	0.45
		5.41	0.60
C9 C6H	7.40	7.33	0.07
		7.05	0.35
C9 C5H	5.49	5.49	0.00
		5.36	0.13
C9 C1′H	5.57	5.36	0.21
G10 C8H	7.83	7.76	0.07
G10 C1′H	5.80	5.73	0.07
C11 C6H	7.26	7.26	0.00
C11 C5H	5.38	5.34	0.04
G12 C8H	7.88	7.88	0.00

All the exchange cross-peaks observed arise from DNA resonances; the absence of exchange cross-peaks for drug resonances indicates that distamycin has only a single mode of binding to the dodecamer and that, under the conditions used, virtually all distamycin molecules are bound to DNA. The fourth type of cross-peak in the exchange spectrum occurs between (formerly) symmetry related pairs of drug-bound DNA resonances. While these peaks indicate the occurrence of another exchange process, we show later that this exchange is still the result of a single mode of binding.

Assignments of the Exchangeable Protons: NOEs in H_2O. Since both distamycin and DNA contain exchangeable protons, experiments were performed in H_2O solution to observe the resonances of drug amide and DNA imino protons. Due to its 2-fold symmetry, the original dodecamer spectrum contained two AT imino resonances and the internal three GC imino resonances (Patel, 1982). Figure 3 shows the spectrum of dodecamer to which 1.0 equiv of drug has been added. As expected, there are now four imino resonances due to AT base pairs (labeled a–d) in the assymetric complex. Three new peaks (h–j) appear between 8.8 and 11 ppm and can be assigned to the exchangeable protons of the drug (four amides plus the two terminal NH_2 groups). Judging by intensities, peaks h and i are due to single protons, while peak j appears to contain three or four protons. In the spectrum of free distamycin in H_2O at 10 °C (not shown), there are also three amide peaks in the 8–10 ppm region, at 8.2 ppm (intensity = 1), 9.1 ppm (intensity = 2), and 9.8 ppm (intensity = 1). The terminal NH_2 resonances appear as broad peaks at 8.4 and 8.8 ppm. The most downfield amide in the free drug spectrum is assigned to NH-1 (see Figure 1 for numbering scheme) as it gives a strong NOE to the formyl proton at 8.1 ppm.

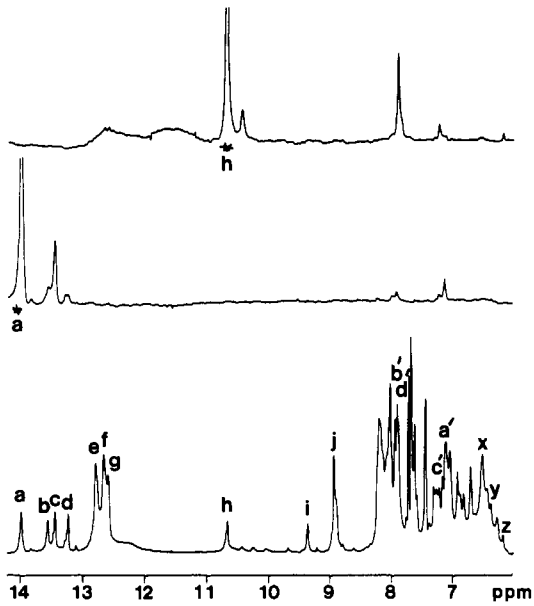

FIGURE 3: Spectrum of the exchangeable protons of the distamycin–DNA complex. The spectrum shown on the bottom was obtained from a 1:1 complex of distamycin–DNA in H_2O. Two representative NOE difference spectra are shown: the middle spectrum was obtained by saturating imino resonance a; the top spectrum was obtained by saturating amide resonance h.

Table II: Summary of NOEs Observed in H_2O for the Distamycin–DNA Complex

peak irradiated	NOEs obsd	peak irradiated	NOEs obsd
imino a	C2H a′, d′, c′, b′	amide h	C2H c′, H3 z
imino b	C2H b′, d′, c′, a′	amide i	C2H b′, H3 z, x
imino c	C2H c′, b′, d′, a′	amide j	C2H d′, a′, H3 x, y
imino d	C2H d′, b′		

In order both to assign the resonances and to look for drug–DNA contacts, steady-state NOE experiments were performed. Two representative NOE difference spectra, one in which at AT imino proton was irradiated and one in which a drug amide proton was irradiated, are shown in Figure 3. The results of all the NOE experiments are summarized in Table II. Assignment of the DNA imino protons could not be accomplished solely on the basis of imino-to-imino NOEs due to the appearance of exchange-mediated saturation-transfer effects. Peaks in the difference spectra due to saturation transfer are easily distinguished from NOE peaks by their high intensity. For example, irradiation of imino peak a resulted in saturation transfer to imino peak c. The presence of this exchange phenomenon further complicates matters since exchange-transferred NOEs may also be observed. The fact that all four adenine C2H resonance appear in the difference spectrum labeled a further documents this exchange process since it is impossible to get direct NOEs from one AT imino proton to all four adenine C2 protons. In spite of these complications, it is possible to unambiguously assign the exchangeable proton spectrum. Irradiation of each AT imino peak separately resulted in a major NOE to an adenine C2H as well as two or three minor C2H NOEs, and the major NOE was therefore assigned to its own C2H (labeled correspondingly a′–d′). We have already identified the C2H resonances from the 2D exchange experiments described above: the two upfield C2H peaks (a′ and c′) are derived from A5 (i.e., A5 and A17), and the two downfield peaks (b′ and d′) are derived from A6 (i.e., A6 and A18). Thus, the imino peaks that show pairwise saturation transfer, namely, a with c and b with d, are symmetry-related. This exchange behavior is identical with the fourth (i.e., flip-flop) type of exchange cross-peak observed in the 2D experiments described above. Although the GC imino protons are not well resolved in the spectrum of the drug–DNA complex, it was not neccessary to assign these peaks in this study.

Irradiation of each of the drug amide peaks (labeled h–j) gives rise to both intramolecular and intermolecular NOEs. The intramolecular NOEs were used to assign the amide and pyrrole H3 peaks of the drug molecule while the intermolecular NOEs were used to assign the AT imino and adenine C2H peaks of the asymmetric DNA strands. All the observed NOEs are negative, indicating that the drug molecule is tumbling with the correlation time of the larger DNA molecule, confirming that the drug molecule is tightly bound to the DNA dodecamer. Intramolecular NOEs are observed between each amide proton and a pyrrole proton resonating between 6 and 7 ppm (x–z), identifying the latter as the three pyrrole H3 resonances. (Although these protons are not fully excited by the Redfield pulse used, the NOEs between them and the amides are clearly visible.) Peak h gives an NOE to peak z and a strong NOE to a sharp resonance at 8.1 ppm, which can be assigned to the terminal formyl proton of the drug. Therefore, peak h is assigned to NH-1, and peak z is assigned to the H3 of pyrrole ring 1. Peak i also gives an NOE to peak z as well as to peak x. Therefore, i is assigned to NH-2, and x is assigned to the H3 of pyrrole ring 2. The NOE difference spectrum for peak j, which contains several protons, contains a somewhat broad peak at ~8.2 ppm whose intensity is too high to be due to an NOE and must therefore be due to a saturation-transfer event. This occurs between the two terminal NH_2 groups, which resonate at 8.2 and 8.9 ppm (peak j) and can exchange chemical shift identities following a 180° rotation about the C–C bond. Peak j also gives NOEs to pyrrole peaks x and y. Therefore, j contains NH-3 and NH-4 in addition to an NH_2, and y is assigned to the H3 of pyrrole ring 3. This completely assigns resonances for the protons on the concave side of the curved drug molecule.

Defining the Binding Site. The binding configuration was established from the intermolecular NOEs observed between distamycin and the DNA. Each of the drug amides gives an NOE to an adenine C2H resonance, confirming that the drug is binding in the minor groove of the B-form DNA duplex. Peak h (NH-1) gives an NOE to one of the A5-derived C2H peaks (c′), peak i (NH-2) to C2H b′, and peak j (NH-3 or -4) to C2H d′. Once we arbitrarily assign a single C2H to a particular strand, there is only one way to consistently assign the rest. For example, if C2H peak a′ is A17, then C2H peak c′ must be A5, which is in contact with the NH-1 of the drug molecule. NH-2 is in contact with C2H b′, which must be the nearest neighbor to A5, i.e., A6, which then leaves C2H d′ as A18. Figure 6 schematically places the distamycin molecule in the minor groove of the DNA in the configuration that is consistent with all the NOE results, with C2H a′ called A17. It is immediately obvious from the picture that if we had chosen to designate C2H a′ as A5 rather than A17, we would end up with exactly the same binding site. The observation of strong NOE cross-peaks in the NOESY spectrum (see below) between each of the three pyrrole H3 resonances and an adenine C2H resonance confirms this conclusion.

Structural Aspects of the Complex: NOESY Experiments. In order to obtain further information about the structure of the drug–DNA complex, NOESY spectra were obtained in D_2O solutions. Our original intent was to analyze the NOESY spectra quantitatively to detect differences in the conformation

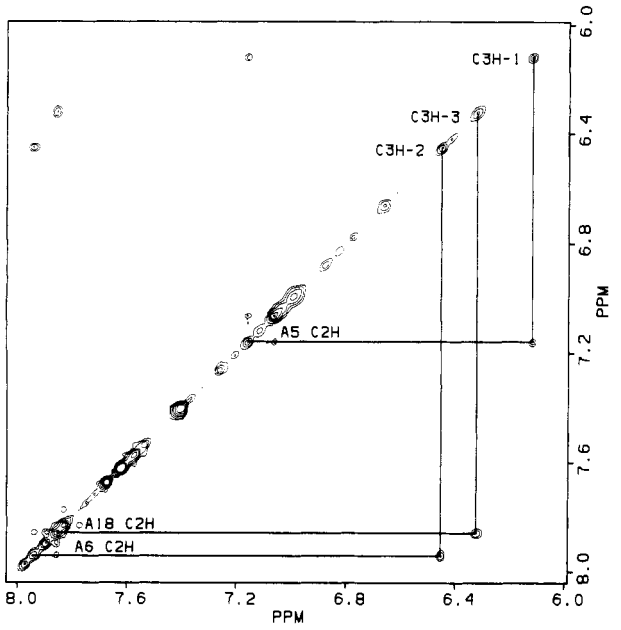

FIGURE 4: NOESY spectrum of the distamycin–DNA complex: the aromatic-to-aromatic region of a NOESY spectrum obtained with a mixing time of 300 ms at 17 °C.

of the DNA that might occur as a result of drug binding. However, the spectra obtained could not be analyzed in this manner for three reasons. First, unlike the 2D spectrum of the dodecamer alone, the spectrum of the complex suffers greatly from spectral overlap in both the C1′H region and the C2′H, C2″H region. Second, many of the cross-peaks in the NOESY spectra of the complex have extremely low intensities. Third, under some conditions the NOESY spectrum was complicated by the presence of cross-peaks due to exchange and exchange-transferred NOEs. While these effects could make assigning the spectrum difficult, the problem was circumvented by obtaining the assignments from the exchange spectrum, as described above. As was the case with assigning the resonances from the H_2O NOE experiments, strand-specific assignments can be made in only one internally consistent manner relative to the drug molecule. Since, in some instances, it was neccessary to go down close to the noise level to detect the cross-peaks, several NOESY experiments were performed to ensure the occurrence of these cross-peaks. Even so, the low cross-peak intensities made it impossible to analyze the data quantitatively. Since there are several phenomena that can cause the loss of NOE intensity (for example, peak broadening), the cross-peak intensities are interpreted only qualitatively.

Despite the difficulties mentioned above, the NOESY spectra of the distamycin–DNA complex contain much useful information regarding both intermolecular contacts and the conformation of the DNA molecule. There are several cross-peaks due to contacts between drug and DNA protons, which are shown in Figure 4. Three strong intermolecular cross-peaks are observed in the left spectrum: each connects a previously assigned (from the H_2O NOEs) drug pyrrole H3 resonance to an assigned adenine C2H resonance. The correlations observed are H3-1 to A5 C2H, H3-2 to A6 C2H, and H3-3 to A18 C2H; these are exactly those that are predicted from the NOE data obtained in H_2O solution.[2] This spectrum, collected at 17 °C, is completely devoid of cross-peaks due to exchange. However, the intramolecular DNA NOE peaks are extremely weak in this spectrum, making it particularly difficult to analyze. Thus, it was neccessary to go to longer mixing times (to increase the cross-peak intensity) or higher temperatures (to rearrange the chemical shift overlaps) to obtain stronger and better-resolved cross-peaks.

[2] N.B. From this point on, the numbering scheme for the DNA duplex is for the asymmetric dodecamer, i.e., strand 1, residues 1–12, and strand 2, residues 13–24.

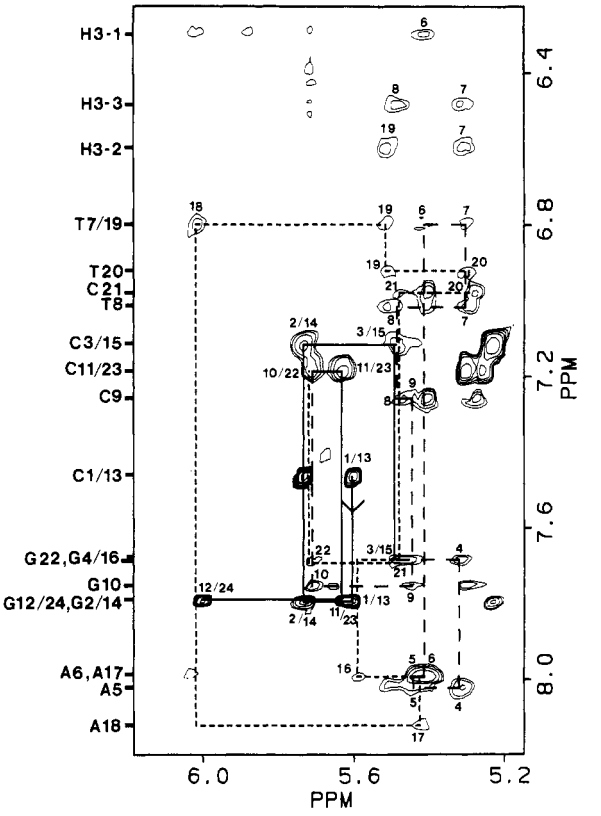

FIGURE 5: NOESY spectrum of the distamycin–DNA complex: the aromatic-to-C1′H region of a NOESY spectrum obtained with a mixing time of 300 ms at 27 °C. The assignments of the aromatic resonances (i.e., the C6H's of cytosine and thymine and the C8H's of guanine and adenine) are along the left axis, while the numbers above the cross-peaks denote the C1′ assignments. Those resonances that correspond to both members of a formerly symmetry related pair are denoted as C1/13, whereas those peaks that contain overlapping resonances are denoted as A6, A17. The solid lines follow the sequential connectivities through the resonances that still possess chemical shift symmetry in the complex, and the two dashed lines follow the connectivities along each of the strands through the resonances that have lost their symmetry due to drug binding.

The spectrum in Figure 5 shows a region of a NOESY spectrum obtained at 27 °C. Under the conditions of this experiment, cross-peaks due to exchange appear, but there is little evidence of exchange-transferred NOEs. Since the exchange cross-peaks all occur very near to the diagonal (see Figure 2), they do not hinder the analysis of other regions of the 2D spectrum. The region shown includes cross-peaks due to NOEs between aromatic protons (both DNA and distamycin) and C1′ protons. Due to the loss of symmetry caused by drug binding, the sequential connectivities for DNA resonances must now be followed separately along each of the two strands. The strands cannot be unambiguously assigned as residues 1–12 or 13–24 solely on the basis of the sequential connectivities. Strand-specific assignments are made possible, however, by taking advantage of the intermolecular NOEs observed between (assigned) distamycin pyrrole H3 resonances and C1′H resonances. From these NOEs (see Figure 5), it is possible to distinguish between the formerly symmetry related C1′H resonances in only one way that is internally consistent with the binding site assignments made above. For

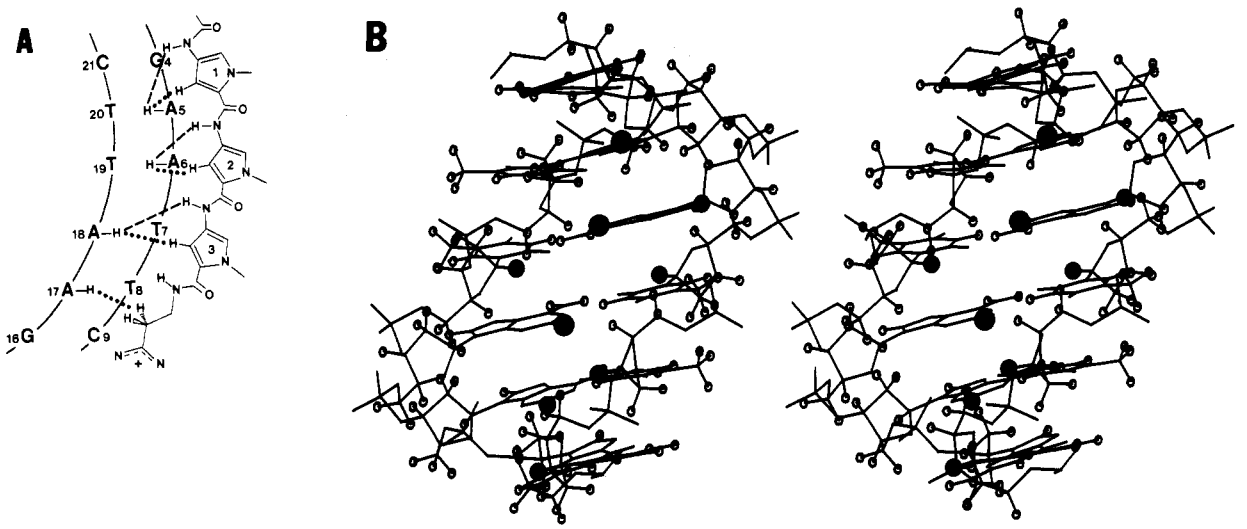

FIGURE 6: The distamycin binding site. (A) Diagrammatic representation of the distamycin binding site in the central AATT region of d(CGCGAATTCGCG)$_2$. The observed NOE contacts from assigned adenine C2H resonances to distamycin amide protons (dashed lines) and to nonexchangeable distamycin protons (dotted lines) are indicated. (B) Stereo view of the DNA duplex from the direction of approach of a drug molecule, showing the access into the distamycin binding site in the minor groove. The right strand shows, from top to bottom, residues G4–A5–A6–T7–T8–C9 with the left strand, from bottom to top, showing residues G16–A17–A18–T19–T20–C21. The three adenine C2H atoms that show strong NOE contacts with the three pyrrole H3 atoms and weaker NOEs to the three amide protons in distamycin are shown as large filled spheres. Additional NOEs between distamycin H3 protons to DNA 1′ protons, as well as the C2H of A17 that shows an NOE to the distamycin propylammidinium group (bottom), are indicated by smaller filled spheres.

example, pyrrole H3-1 gives a single cross-peak in this region to the C1′H of either A6 or A18, and it gives a strong NOE to the C2H of A5 (see Figure 4). Since A6 is adjacent to A5 while A18 is two residues away and on the opposite strand from A5, the C1′H resonance that gives an NOE to pyrrole H3-1 must be that of A6. Similarly, pyrrole H3-3 gives cross-peaks to two C1′H resonances, one of which is either T8 or T20 and the other of which is either T7 or T19, and to the C2H of A18. Again, on the basis of the binding site geometry (see Figure 6), the two C1′H resonances that give NOEs to H3-3 must be from T8 and T7, rather than from T20 and T19. Finally, pyrrole H3-2 gives NOEs to the C1′H resonances of both T7 and T19, as well as to the C2H of A6. There are two other intermolecular NOEs observed in other regions of the NOESY spectrum. The C2H resonance of A17 gives cross-peaks to two resonances at 3.53 and 3.33 ppm. These two resonances give strong cross-peaks to each other and are *J*-coupled (as observed in a COSY spectrum) to another such pair of resonances further upfield. These two pairs of peaks can only belong to the four methylene protons of distamycin. The downfield methylene protons also give NOESY cross-peaks to one of the C1′H resonances of the pair C9/C21. Again, on the basis of the established binding site geometry, the C1′H involved must be from C9. The relationships between C1′ protons and C2 protons can be visualized in the stereo diagram in Figure 6. The intermolecular NOEs, summarized in Table III, are illustrated in Figure 6 and further define the binding site suggested on the basis of the NOEs observed in H_2O.

With strand-specific assignments established for several C1′H resonances, it is now possible to identify the sequential connectivities along the two strands of DNA in the complex, as presented in Figure 5. As was evident from the exchange spectra, the resonances from residues near the ends of the dodecamer are superimposed, indicating little perturbation from their original 2-fold symmetry; the individual strand connectivities begin with the fourth residue (in the 5′–3′ sense) and end at the eleventh residue. As mentioned earlier, many of the intramolecular NOEs that are expected to appear for normal B-form DNA are either very weak or missing, but the assignments are already well-established from the exchange spectrum. In the sequential walk along strand 1 (residues 1–12) all the internucleotide cross-peaks expected for normal B-DNA are present, although the nearest-neighbor NOE from the T7 C6H to the A6 C1′H is very weak. On strand 2 (residues 13–24), several abnormalities in the connectivities, and presumably in the DNA structure, are observed. The intraresidue NOEs between the C8H and C1′H of residues G16 and A18 are missing from the NOESY spectrum, and the C6H to C1′H cross-peak of C21 is extremely weak. In addition, the nearest-neighbor NOE between the C6H of C21 and the C1′H of T20 appears to be missing, although it may lie under the cross-peak due to the C6H to C5H NOE of C21. Two anomalous cross-peaks are observed for strand 2 in the aromatic-to-C1′H region of the NOESY spectrum obtained at 17 °C, where the resonance positions of the C8H's and C2H's of the adenines are shifted slightly. The C2H of A18 gives cross-peaks to the C1′H resonances of T7 and T8. Also in the low-temperature spectrum, anomalous cross-peaks appear between the C2H of A6 and the C1′H resonances of T19 and T7. Due to badly overlapping resonances in the C2′H, C2″H region, it is difficult to draw many conclusions from this part of the spectrum. There are, however, a few anomalous cross-peaks that can be unambiguously assigned: the methyl resonance to T20 gives NOEs to both the C6H and C5H of C21.

Table III: Summary of Intermolecular NOEs for the Distamycin–DNA Complex

drug proton	DNA proton	drug proton	DNA proton
NH-1	A5 C2H	NH-3	A6 C2H
H3-1	A5 C2H		A18 C2H
	A6 C1′H	H3-3	A18 C2H
NH-2	A5 C2H		T7 C1′H
	A6 C2H		T8 C1′H
H3-2	A6 C2H	CH_2	A17 C2H
	T19 C1′H		C9 C1′H
	T7 C1′H		

Dynamics of the Distamycin–DNA Complex. The observation in Figure 1 that, at substoichiometric ratios of drug: DNA, the NMR spectrum contains resonances from unbound

DNA dodecamer as well as resonances from the drug–DNA complex indicates that the complex is in slow exchange with free DNA on the NMR time scale. The limiting behavior for slow-exchange behavior from a chemical shift standpoint is $k_{ex} \ll |\Delta\omega|$. At 27 °C, the smallest chemical shift difference between the free and bound forms is 15 Hz (for the methyl resonance of T8). Since the binding constant of distamycin A, K_{app}, is around 10^7 M^{-1} (Gursky et al., 1982), k_{on} is much greater than k_{off}, and k_{ex} is essentially a measure of k_{off}, which is therefore much slower than 15 s^{-1}. A more accurate value for k_{off} can be obtained from a 2D exchange experiment done with a short mixing time. For a τ_M of 50 ms, the average integrated intensity of an exchange cross-peak relative to its corresponding diagonal peak is 0.2. Since the spectrum obtained with a 50-ms mixing time contained almost no NOE cross-peak intensity, it is reasonable to use the diagonal peak intensities as very little cross relaxation has occurred during the short mixing time. Thus, the ratio of intensity can be interpreted as indicating that 2 out of 10 complexes have dissociated in 50 ms, indicating that k_{off} is ~ 4 s^{-1}. Since this value was obtained without correcting for relaxation processes that may have occurred during the mixing time, it can be taken as an upper limit of k_{off}. A more accurate determination of the exchange rate would require obtaining a series of exchange spectra with mixing times shorter than the 50 ms used (Jeener et al., 1979).

As mentioned earlier, the 2D exchange spectra contain an additional class of cross-peaks that do not correspond to the primary dissociation event. Such peaks are denoted by arrows in Figure 2. Each cross-peak connects two DNA resonances in the complex that were originally derived from a symmetry-related pair (e.g., A5 and A17, A6 and A18, etc.). There are, however, no exchange cross-peaks observed for drug resonance. Thus, the second exchange event does not result in a change in chemical environment for the drug molecule. Since the two strands in the DNA duplex only have separate identities as a consequence of drug binding, these cross-peaks must involve DNA molecules that have formed a complex. Taken together, these observations indicate that the cross-peaks arise when, during the experimental mixing time, a drug–DNA complex that has the drug bound to strand 1 becomes a complex that has the drug on strand 2. This can be represented by a first-order exchange mechanism in which the drug molecule remains loosely bound to the DNA but rearranges itself to become associated with the opposite strand of the same DNA molecule. Since the net result of this process can be represented by a drug molecule flipping head-to-tail on a single DNA molecule, we will designate these cross-peaks as "flip" cross-peaks to distinguish them from the primary cross-peaks that arise from a simple dissociation event.

The rate at which the flipping process occurs can be estimated by the buildup rate of the flip cross-peaks as a function of mixing time. The rate of this first-order process is dependent only on the concentration of drug–DNA complex, which is a constant under the experimental conditions, and therefore the buildup rate is expected to approach its limiting value exponentially, with a time constant of k_{flip}. (The intensity of the flip cross-peaks relative to their corresponding diagonal peaks should approach 0.5 since only half the reassociation events will result in a flip.) Exchange experiments with τ_M of 50, 100, and 400 ms were performed on a sample of dodecamer to which 0.5 equiv of distamycin A had been added. Since, at intermediate and long mixing times, the intensities of diagonal peaks will be low due to cross relaxation mechanisms, the average intensities were compared by the ratio of flip intensity:exchange intensity. Within the experimental error, this ratio was constant over the range of mixing times used, at a value of about 0.5 ± 0.05. Thus, a distamycin molecule flips on a DNA duplex at half the frequency at which it dissociates. This observation yields a k_{flip} of ~ 2 s^{-1}.

Discussion

There has been much interest over the years in understanding the nature of the interactions between DNA and small molecules. The minor groove binding drugs netropsin and the related distamycin A have been used as model systems to study the nature of sequence-specific binding. Until recently, the most widely accepted model specified that intermolecular hydrogen bonds between the amide protons on the concave edge of the drug molecules and H-bond acceptors, such as the O2 of thymines, were responsible for the sequence specificity. However, the X-ray crystal structure of a complex between netropsin and the same symmetric DNA dodecamer that we have studied strongly suggested that the important contacts are actually van der Waals interactions between the aromatic pyrroles of the drug and adenine rings (Kopka et al., 1985). In the crystal structure, the hydrogen bonds that were suggested on the basis of model building (Gursky et al., 1977) appear to be bifurcated and longer than normal hydrogen bonds and are thus assumed to play a more minor role than originally believed. These results show the importance of making physical measurements in order to test a hypothesis based on model building. Dickerson and co-workers have extended their results with netropsin to infer a structure of the complex between the longer distamycin molecule and DNA. The NMR studies reported here have allowed us to determine the structure of the distamycin complex as well as to gain information about the dynamics of the interctions in solution.

One-dimensional NOE experiments in H_2O and two-dimensional experiments in D_2O have resulted in the observation of many intermolecular proton–proton contacts (Table II). All these contacts can be accounted for in a unique binding site on the DNA duplex. By far the strongest NOEs are from the interactions between pyrrole H3's and adenine C2H's, identifying these protons as the points of nearest contact between the drug and DNA. Figure 6B shows the geometry of the four adenine C2H's as they would appear to the drug prior to binding. There is a one-to-one correspondence between the drug pyrrole rings 1, 2, and 3 and the adenine bases A5, A6, and A18 respectively, in the complex. The DNA sequence studied here contains another stretch of three continuous adenines, namely, A6–A18–A17. Although the three pyrrole rings of distamycin could also interact with this sequence, the studies here show that there is a strong preference for the former site. The binding geometry shown in Figure 6A reveals that the propyl chain at the ammidinium end of distamycin interacts with the C2H of A17. In the alternate binding site, i.e., the one in which the drug molecule is displaced by one residue down the DNA, the propyl chain would be opposite C9–G16, which is likely to be less favorable on steric grounds. We do observe some low-intensity resonances in the spectra of the distamycin–DNA complex that we believe are due to a small amount of this alternate form, but judging from the intensities of the peaks, this form represents less than 10% of the complex.

The binding of distamycin A to the symmetric dodecamer results in changes in chemical shifts for a majority of the assigned resonances (Table I). Although it is dangerous to try to infer precise structural features on the basis of chemical shift changes, it is clear from the magnitude of these changes,

and from the sequential connectivities, that not all the changes can be due to ring current shift effects from the aromatic drug molecule itself, and thus some rearrangements in the DNA structure have apparently taken place. Our hope was to be able to determine precisely what these changes are by careful analysis of the NOESY spectra. Although this goal could not be accomplished due to technical reasons, the anomalous NOEs observed can be used to draw some conclusions. On the basis of the number of anomalous obervations, it appears that strand 1 of the complex is more distorted from normal B form than is strand 2. The region affected extends from G4 through C9. Two of the three intermolecular van der Waals contacts in the complex are on strand 1. The disappearance of intraresidue and interresidue NOEs between base protons and sugar C1′ protons could be caused by a change in propeller twist, base roll, or helical twist. The anomalous NOEs observed between base protons of T20 and C21 are probably due to a change in base roll of one or both of the base pairs, bringing these protons closer together in the major groove. In the crystal structure of the dodecamer (Drew & Dickerson, 1981), the distances from the T20 CH_3 to the C21 C5H and C6H are 5.0 and 6.8 Å, respectively. The observation of such cross-peaks in the NOESY spectra indicates that these distances are now closer than 4 Å. The consequence of such a change would be greater separation between the edges of the two bases in the minor groove. There are no proton–proton contacts observed between the drug molecule and C9. However, this is the region of the DNA molecule where the formyl end of the drug must reside, and such an adjustment may help to make room for this group in the minor groove.

Although the results reported here for the distamycin–DNA complex agree in general with the crystal results for the netropsin–DNA complex, there are significant differences. The polarity of binding to the symmetric dodecamer is the same for the two drugs. On the other hand, the largest perturbation in DNA conformation observed in the netropsin–DNA complex occurs at the step T8–C9, where large changes are observed in the local helical twist angle, the rise per base pair, and the base roll angle (Kopka et al., 1985). The authors conclude that these changes are caused by the insertion of the propyl chain at the ammidinium end of the netropsin molecule between T8 and C9. The conformational perturbation observed at the step T20–C21 in the distamycin–DNA complex is very similar in nature, but it is caused by the insertion of the other end of the distamycin A molecule. (Both netropsin and distamycin contain propylammidinium groups at one end, while netropsin has a guanidinium group and distamycin has a formamide group at the other end.) Furthermore, on the basis of the netropsin crystallographic results, the binding site for the longer distamycin A molecule has been predicted (Kopka et al., 1985). In agreement with the model proposed by Schulz and Dervan (1984), the optimal binding site predicted by Kopka and co-workers for distamycin is five base pairs rather than the four for netropsin. However, our results show that the four base pair sequence 5′-AATT-3′ is already a perfectly good binding site for distamycin. In fact, the addition of a fifth AT base pair results in a DNA molecule that possesses two distamycin binding sites of approximately equal affinity (unpublished observation).

Despite the use of NOEs in only a qualitative manner, it is clear that 2D NMR studies of the type described above can define the structure of liganded DNA complexes with remarkable precision. We hope, with the use of more quantitative distances derived from time-dependent NOEs, combined with computer methods based on distance geometry algorithms (Crippen et al., 1981), to eventually be able to determine such structures in solution at atomic resolution. We are currently investigating distamycin complexes with different but related central AT sequences to better understand the forces responsible for the sequence specificity of the high-affinity binding of the drug to DNA molecules.

ACKNOWLEDGMENTS

We thank Dr. Agustin Kintanar for his helpful suggestions and critical reading of the manuscript.

REFERENCES

Crippen, G. M., Oppenheimer, N. J., & Connolly, M. L. (1981) *Int. J. Pept. Protein Res. 17*, 156–169.

Gursky, G. V., Tumanyan, V. G., Zasedatelev, A. S., Zhuze, A. L., Grokhovsky, S. L., & Gottikh, B. P. (1977) *Nucleic Acid–Protein Recognition* (Vogel, H. J., Ed.) p 189, Academic Press, New York.

Gursky, G. V., Zasedatelev, A. S., Zhuze, A. L., Khorlin, A. A., Grokhovsky, S. L., Streltov, S. A., Surovaya, A. N., Nikitin, S. M., Krylov, A. S., Retchinsky, V. O., Mikhailov, M. V., Beabealashvili, R. S., & Gottikh, B. P. (1982) *Cold Spring Harbor Symp. Quant. Biol. 47*, 367–378.

Hare, D. R., Wemmer, D. E., Chou, S. H., Drobny, G., & Reid, B. R. (1983) *J. Mol. Biol. 171*, 319–336.

Jeener, J., Meier, B. H., Bachmann, P., & Ernst, R. R. (1979) *J. Chem. Phys. 71*, 4546–4553.

Klevit, R. E. (1985) *J. Magn. Reson. 62*, 551–555.

Kopka, M. L., Yoon, C., Goodsell, D., Pjura, P., & Dickerson, R. E. (1985) *J. Mol. Biol. 183*, 553–563.

Meier, B. H., & Ernst, R. R. (1979) *J. Am. Chem. Soc. 101*, 6441–6442.

Patel, D. J. (1982) *Proc. Natl. Acad. Sci. U.S.A. 79*, 6424–6428.

Schultz, P. G., & Dervan, P. B. (1984) *J. Biomol. Struct. Dyn. 1*, 1133–1147.

States, D. J., Haberkorn, R. A., & Ruben, D. J. (1982) *J. Magn. Reson. 48*, 286–292.